

:Two Ruthenium Complexes Capable of Storing Multiple Electrons on a Single Ligand - Photophysical, Photochemical and Electrochemical properties of $[\text{Ru}(\text{phen})_2(\text{TAPHAT})]^{2+}$ and $[\text{Ru}(\text{phen})_2(\text{TAPHAT})\text{Ru}(\text{phen})_2]^{4+}$.

Ludovic Troian-Gautier,^{†##} Lionel Marcédis,[§] Julien De Winter,[‡] Pascal Gerbaux[‡] and Cécile Moucheron^{†*}

[†] Organic Chemistry and Photochemistry, Université libre de Bruxelles (U.L.B.), 50 Av. F.D. Roosevelt, CP 160/08, B-1050 Bruxelles, Belgium.

[§] Engineering of Molecular NanoSystems, Université libre de Bruxelles (U.L.B.), 50 Av. F.D. Roosevelt, CP 165/64, B-1050 Bruxelles, Belgium.

[‡] Organic Synthesis and Mass Spectrometry Laboratory, Center of Innovation and Research in Materials and Polymers, Research Institute for Science and Engineering of Materials, University of Mons - UMONS, 23 Place du Parc, B-7000 Mons, Belgium.

* Email: ludovic@live.unc.edu, cmouche@ulb.ac.be

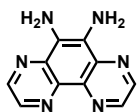
Present Address

Department of Chemistry - Murray Hall, University of North Carolina at Chapel Hill, 123 South Road, Chapel Hill, NC 27599, USA.

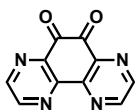
Table of contents

Structures of ligands.....	2
Mass spectrometry.....	3
NMR spectroscopy	7
Photostability measurement.....	9
Infrared spectroscopy	10

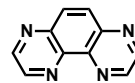
Structures of ligands



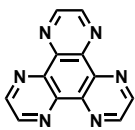
1,4,5,8-tetraazaphenanthrene-9,10-diamine
"diNH₂TAP"



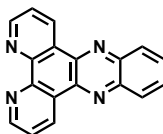
1,4,5,8-tetraazaphenanthrene-9,10-dione
"TAPdione"



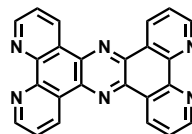
1,4,5,8-tetraazaphenanthrene
"TAP"



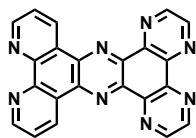
1,4,5,8,9,12-hexaazatriphenylene
"HAT"



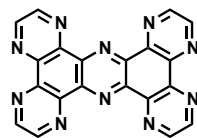
dipyrido[3,2-a:2',3'-c]phenazine
"DPPZ"



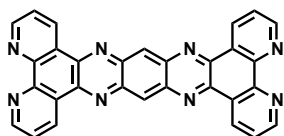
Tetrapyrido[3,2-a:2',3'-c:3'',2''-h:2''',3'''-j]phenazine
"TPPHZ"



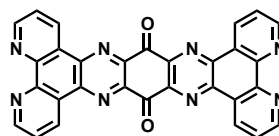
1,10-phenanthroline[5,6-b]1,4,5,8,9,12-hexaazatriphenylene
"PHEHAT"



1,4,5,8-tetraazaphenanthrene[9,10-b]1,4,5,8,9,12-hexaazatriphenylene
"TAPHAT"



9,11,20,22-tetraazatetrapyrido[3,2-a:2',3'-c:3'',2''-l:2''',3'''-n]-pentacene
"TATPP"



9,11,20,22-tetraazatetrapyrido[3,2-a:2',3'-c:3'',2''-l:2''',3'''-n]-pentacene-10,21-quinone
"TATPP"

Figure S1: Structures of the different ligands reported in this study.

Mass spectrometry

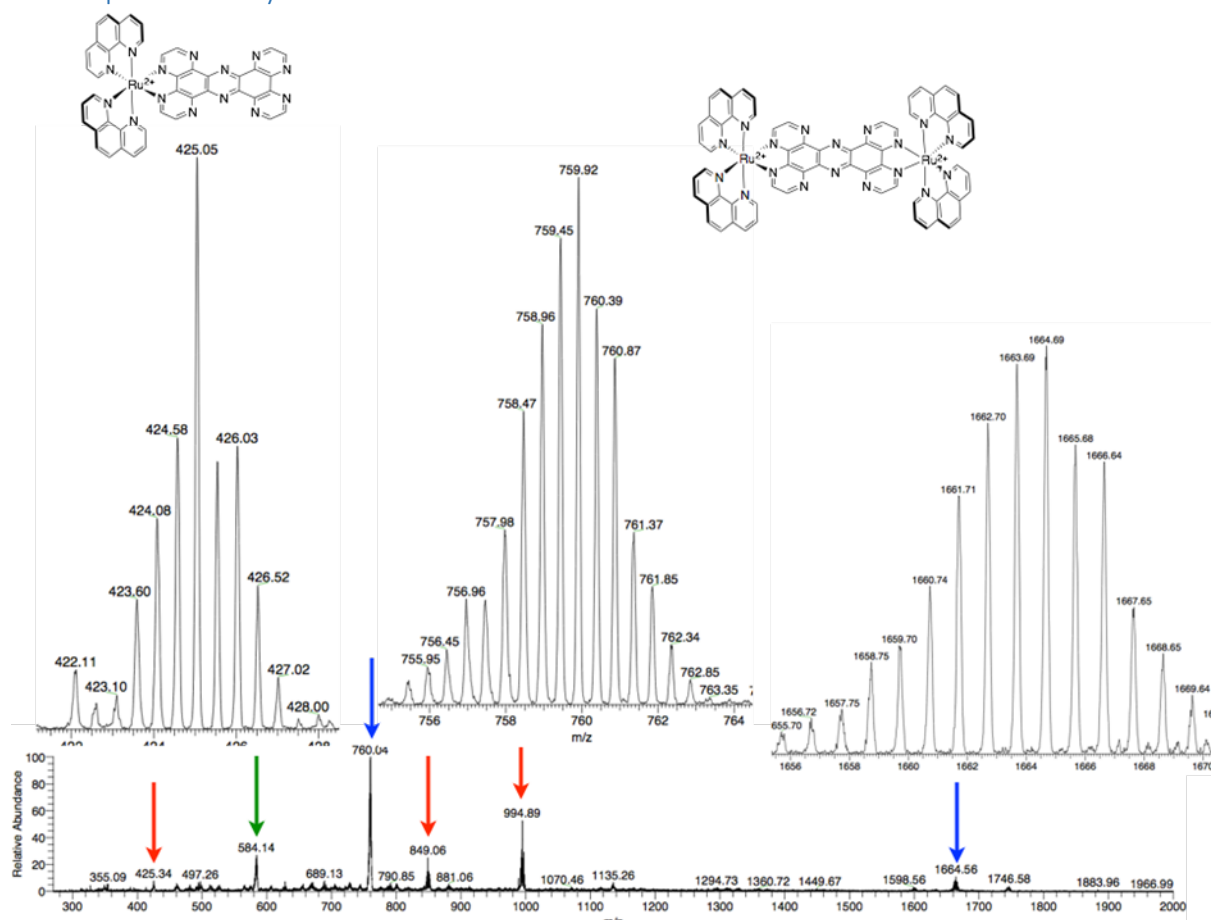


Figure S2: ESI-MS spectrum that shows the formation of mono and dinuclear complexes upon reaction between $[\text{Ru}(\text{phen})_2\text{Cl}_2]$ and TAPHAT. This mixture of products is not obtained when starting from precursor complex $[\text{Ru}(\text{phen})_2(\text{diNH}_2\text{TAP})]^{2+}$ (see below).

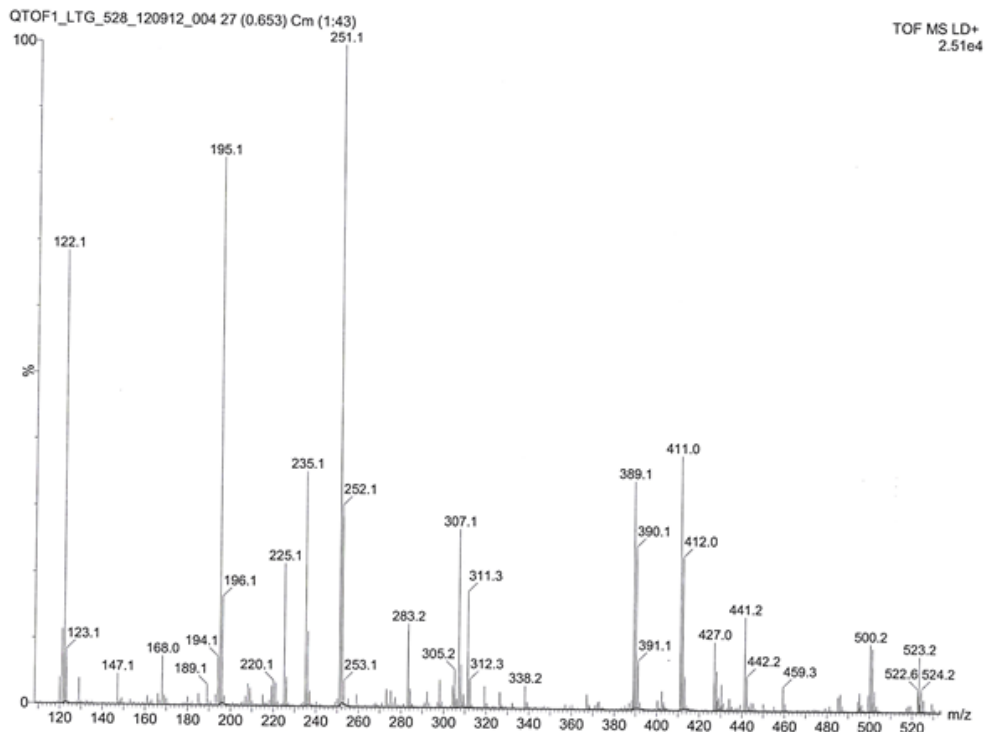


Figure S3: EI-MS spectrum of TAPHAT recorded from THF solutions.

Table S1: Peaks of interest obtained from figure S3. Peaks present at $m/z = 122.1$, 195.1 and 251.1 have not been taken into consideration as they were already present in the neat solvent used for this study.

m/z measured	Attribution	m/z calculated	Relative Intensity
389.1	$[M+H]^+$	389.10	34%
411.0	$[M+Na]^+$	411.08	39%
427.0	$[M+K]^+$	427.06	10%

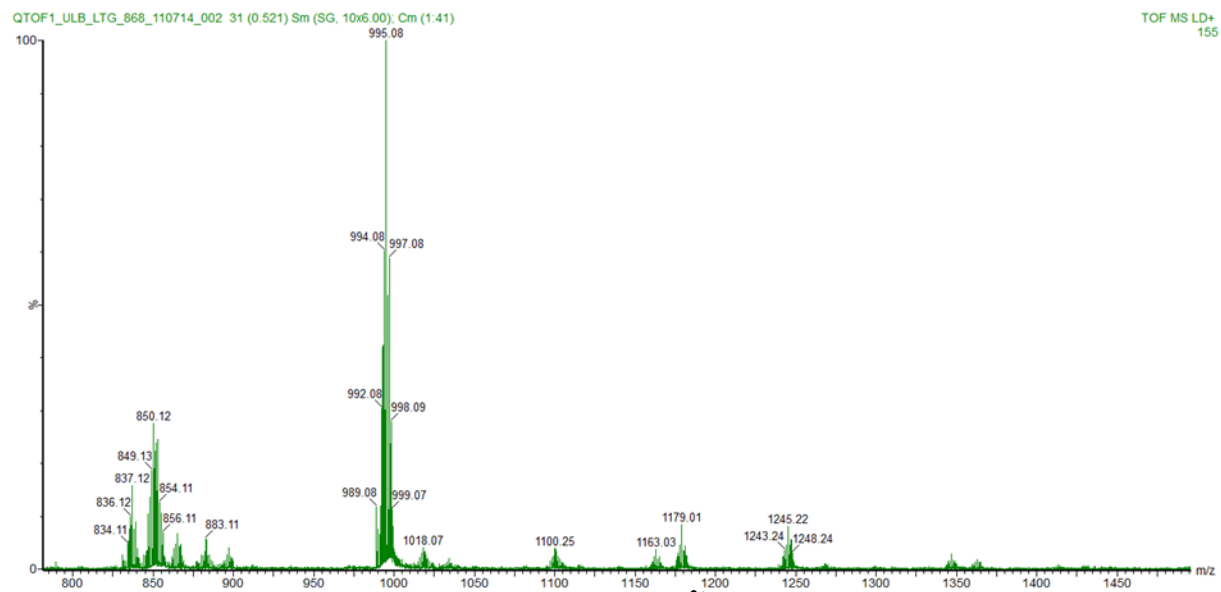


Figure S4: MALDI-MS spectrum of $[\text{Ru}(\text{phen})_2(\text{TAPHAT})]^{2+} \cdot 2\text{PF}_6^-$

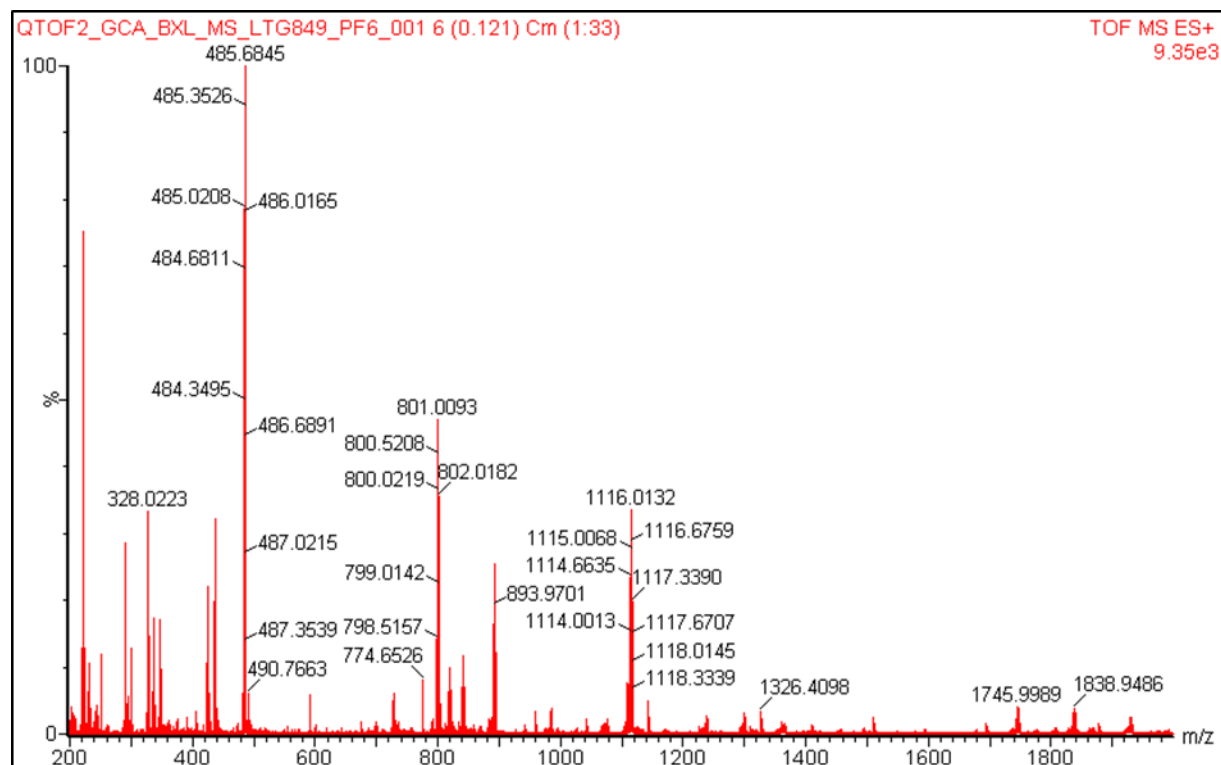


Figure S5: ESI-MS spectrum of $[\text{Ru}(\text{phen})_2(\text{TAPHAT})\text{Ru}(\text{phen})_2]^{4+} \cdot 4\text{PF}_6^-$

Table 5: Peaks of interest obtained from figure S10.

m/z measured	Attribution	m/z calculated	Relative Intensity
328.02	$[\text{M}^{4+}]^{4+}$	328.04	35 %
425.05	$[\text{M}^{4+} - [\text{Ru}(\text{phen})_2]^{2+}]^{2+}$	425.07	22 %
437.03	$[\text{M}^{4+} - \text{H}^+]^{3+}$	437.06	32 %
485.68	$[\text{M}^{4+} + \text{PF}_6^-]^{3+}$	485.38	100 %
801.01	$[\text{M}^{4+} + 2\text{PF}_6^-]^{2+}$	801.05	48 %
893.97	$[\text{M}^{4+} + 3\text{PF}_6^- + \text{K}^+]^{2+}$	893.52	26 %
1116.01	$[2\text{M}^{4+} + 5\text{PF}_6^-]^{3+}$	1116.06	34 %
1746.00	$[2\text{M}^{4+} + 6\text{PF}_6^-]^{2+}$	1746.57	6 %
1838.95	$[2\text{M}^{4+} + 7\text{PF}_6^- + \text{K}^+]^{2+}$	1838.53	6 %
1929.92	$[2\text{M}^{4+} + 8\text{PF}_6^- + 2\text{K}^+]^{2+}$	1930.50	4 %

NMR spectroscopy

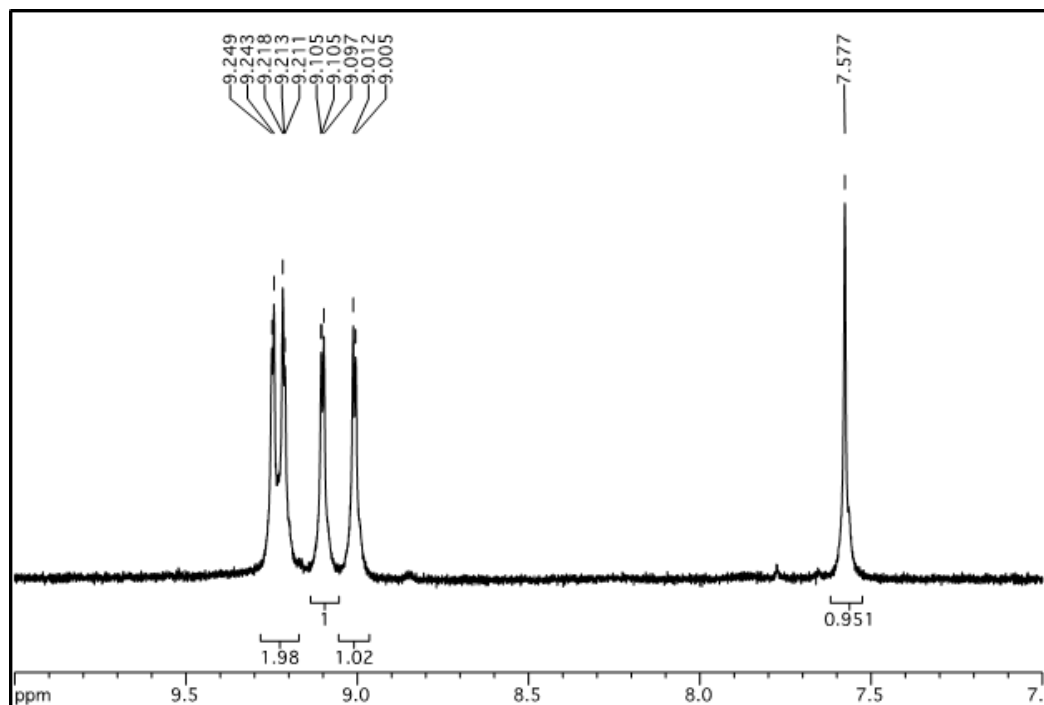


Figure S6: ^1H NMR of 9-hydroxy-1,4,5,8-tetraazaphenanthrene recorded in CD_3OD at 300MHz

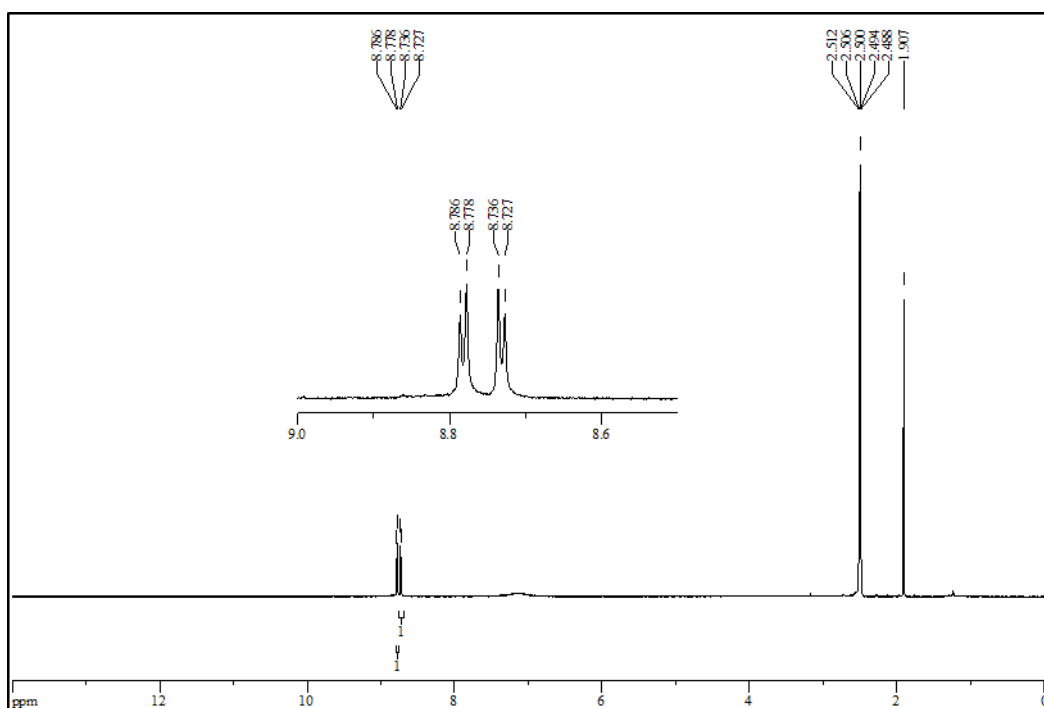


Figure S7: ^1H NMR of 1,4,5,8-tetraazaphenanthrene-9,10-dione recorded in $\text{DMSO}-d_6$ at 300MHz

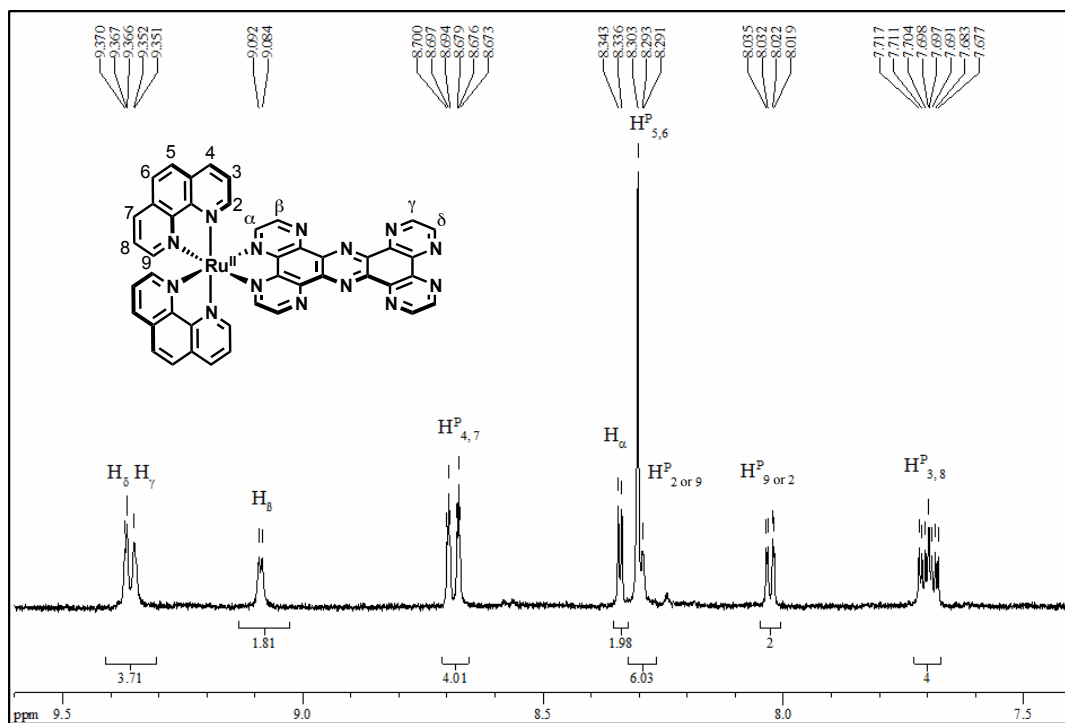


Figure S8: ^1H NMR of $[\text{Ru}(\text{phen})_2(\text{TAPHAT})]^{2+} \cdot 2\text{PF}_6^-$ recorded in CD_3CN at 300MHz

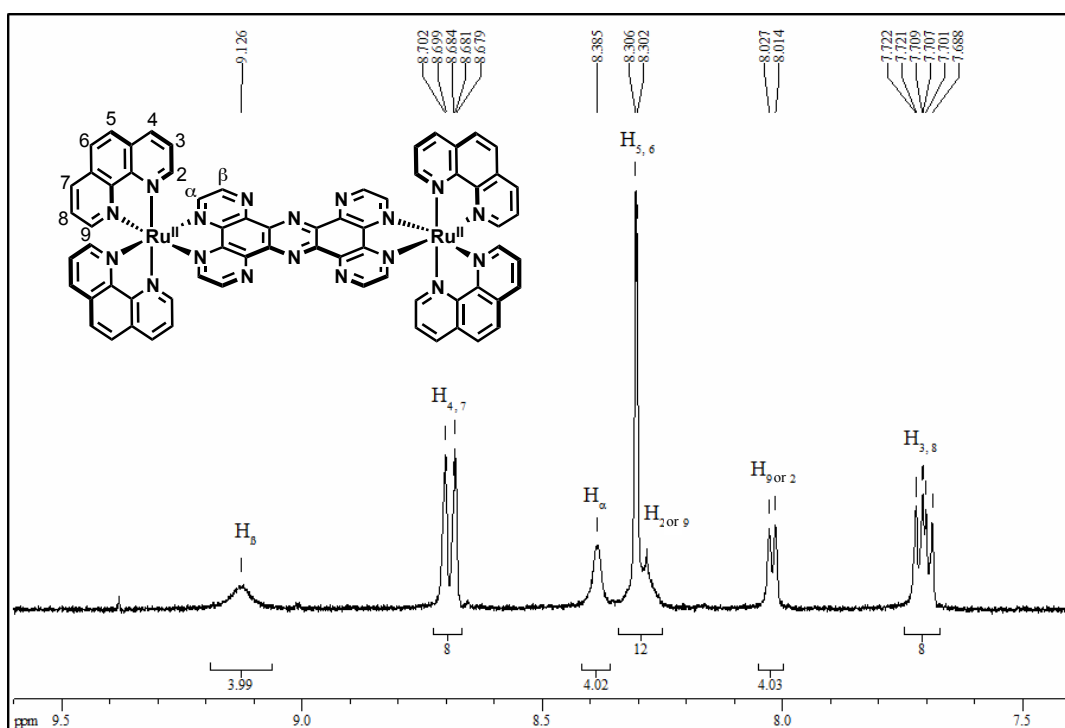


Figure S2: ^1H NMR of $[\text{Ru}(\text{phen})_2(\text{TAPHAT})\text{Ru}(\text{phen})_2]^{4+} \cdot 4\text{PF}_6^-$ recorded in CD_3CN at 300MHz

Photostability measurement

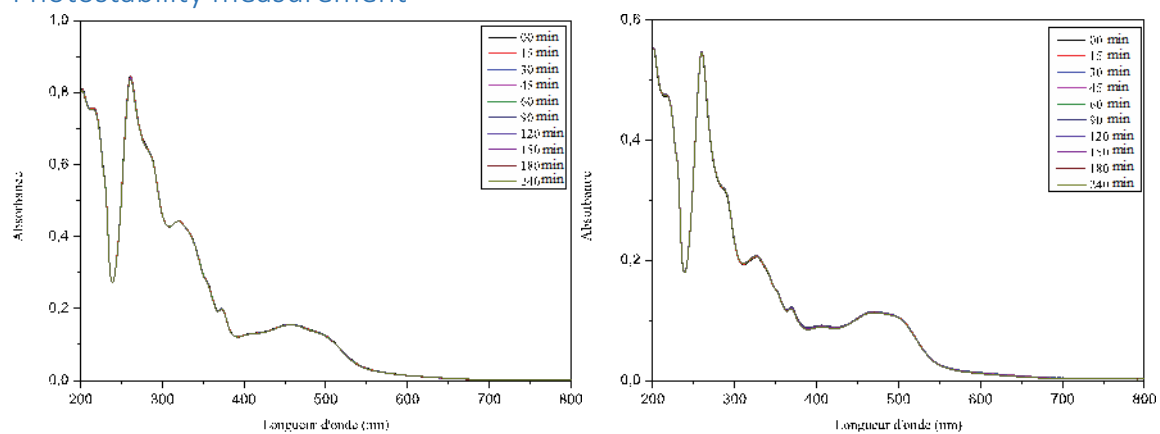


Figure S10: Photostability of $[\text{Ru}(\text{phen})_2(\text{TAPHAT})]^{2+} \cdot 2\text{PF}_6^-$ (left) and $[\text{Ru}(\text{phen})_2(\text{TAPHAT})\text{Ru}(\text{phen})_2]^{4+} \cdot 4\text{PF}_6^-$ (right) under light irradiation (Xe, 200W) in acetonitrile and at room temperature

Infrared spectroscopy

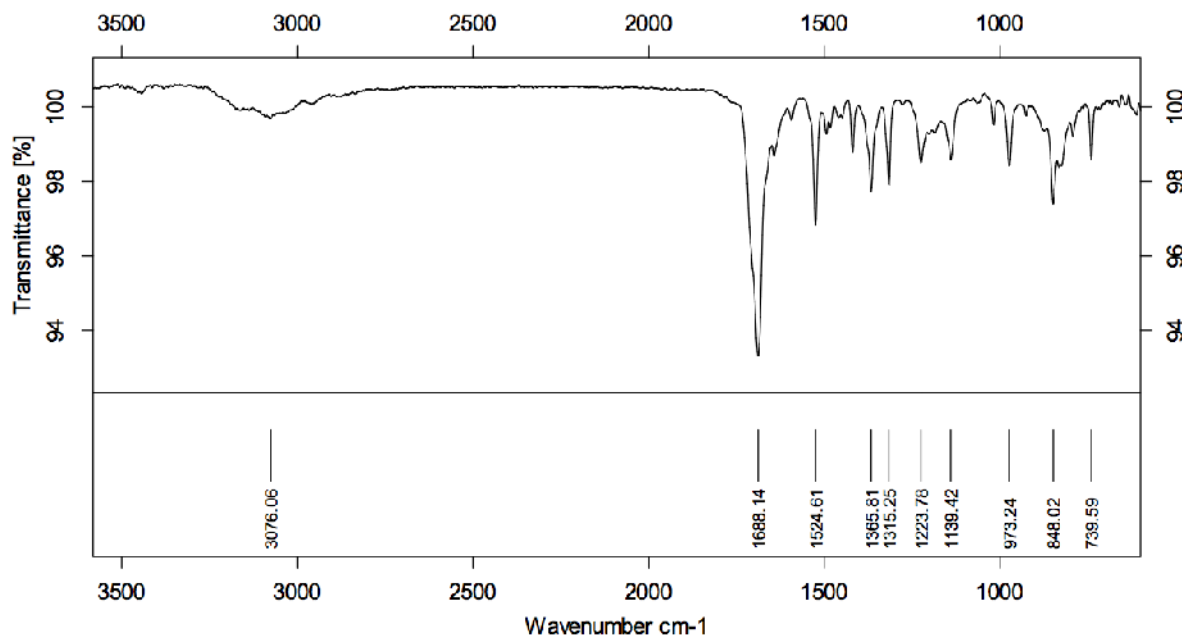


Figure S11: IR spectrum of 1,4,5,8-tetraazaphenanthrene-9,10-dione